Am J Transl Res 2020;12(3):718-730
www.ajtr.org /ISSN:1943-8141/AJTR0101786

Original Article

Inhibition of long non-coding RNA TUG1 protects against diabetic cardiomyopathy induced diastolic dysfunction by regulating miR-499-5p

Lei Zhao[1], Weiguo Li[2], Hao Zhao[3]

Departments of [1]Ultrasonic, [2]Infectious Disease, [3]Pharmacy, Central Hospital of Zhumadian, Zhumadian, Henan Province, China

Received September 2, 2019; Accepted January 22, 2020; Epub March 15, 2020; Published March 30, 2020

Abstract: Reportedly, several long non-coding RNAs (lncRNAs) have been involved in the regulation of cardiac hypertrophy induced by diabetic cardiomyopathy (DCM), causing cardiac dysfunction and subsequent failure. Although lncRNA taurine upregulated gene 1 (TUG1) is associated with myocardial injury, the expression profile and potential role of TUG1 in DCM-related cardiac hypertrophy remain unknown. This study elucidated the functions of TUG1 in DCM and its underlying mechanisms. Our results demonstrated that the expression of TUG1 was upregulated in db/db mice cardiomyocytes. Inhibition of TUG1 by lentivirus si-TUG1 indicated no effect on systolic function; however, it effectively improved DCM-induced diastolic dysfunction in db/db mice. TUG1 silencing demonstrated no influence on the metabolic characteristics of DCM, including blood glucose and lipid levels. Notably, TUG1 knockdown significantly decreased cardiac hypertrophy and reduced the fibrotic area, *in vivo*. To further investigate the underlying mechanism, miR-499-5p was predicted as the targeted TUG1 microRNA. The RT-qPCR and luciferase activity results confirmed that TUG1 negatively regulated miR-499-5p in cardiomyocytes. Furthermore, the overexpression of miR-499-5p abated the inhibitory effects of TUG1 silencing on high glucose-mediated cardiac hypertrophy, *in vitro*. Collectively, our study suggested that TUG1 knockdown attenuated DCM-induced cardiac hypertrophy and diastolic dysfunction by upregulating miR-499-5p. lncRNA TUG1 may be a novel potential target for DCM therapy.

Keywords: Diabetic cardiomyopathy, diastolic dysfunction, cardiac hypertrophy, TUG1, miR-499-5p

Introduction

Diabetic cardiomyopathy (DCM), characterized by the structural and functional impairments of the myocardium, is an important cause of fatalities in patients with diabetes [1]. DCM involves cardiac hypertrophy, fibrosis, and apoptosis and arrhythmias, leading to a global deterioration of cardiac function [2] and is the leading cause of death in DCM. Currently, although various potential mechanisms have been reported in the pathogenesis of DCM, including hyperglycemia, insulin resistance, activation of the renin-angiotensin-aldosterone system, inflammation, and oxidative stress [3], a specific mechanism yet to elucidated [4]. Furthermore, a specific treatment for DCM is still lacking.

Emerging evidence has indicated that long non-coding RNAs (lncRNAs), a subgroup of ncRNAs composed of more than 200 nucleotides [5], are key players in vascular complications associated with diabetes [6]. Studies have reported that lncRNAs are abnormally expressed during the pathogenesis of DCM. Through the lncRNA expression profile analysis in the db/db diabetic mouse model, several hundred of upregulated or downregulated lncRNAs were identified in the myocardium of diabetic mice [7], with some already identified in the development of DCM. For example, lncRNA MALT1 was found to be upregulated in diabetic rats and knockdown of MALT1 has been associated with an improvement in left ventricular systolic function through the alleviation of myocardial inflammation [8]. The knockdown of DCRF in diabetic rats could reduce cardiomyocyte autophagy, attenuate myocardial fibrosis, and improve cardiac function [9]. In addition, Zhang et al. observed that the overexpression of lncRNA CRNDE attenuated cardiac fibrosis and enhanced cardiac func-

tion in DCM mice [10]. These studies suggest the important roles of lncRNAs in the regulation of DCM, necessitating further investigation.

LncRNA taurine upregulated gene 1 (TUG1) was first identified as a part of photoreceptors and retinal development in mouse retinal cells. Recent studies have demonstrated that TUG1 was involved in the development of several malignancies [11-13]. Moreover, it has been reported to regulate myocardial injury, both in vivo [14] and in vitro [15]. Inhibition of TUG1 could prevent myocardial ischemia-reperfusion injury following acute myocardial infarction [14]. Notably, TUG1 also participated in the development of diabetic nephropathy [16]. Collectively, these reports demonstrated that TUG1 plays an important role in the cardiomyocyte (CM) injury and diabetic complications. However, the expression and mechanisms of TUG1 in DCM-induced cardiac hypertrophy remain unknown. Therefore, the present study investigated the involvement of TUG1 in the pathology of DCM and elucidated the potential mechanisms.

Materials and methods

Animals and treatments

Leptin receptor-deficient (db/db) C57BLKS mice and wild-type (wt) C57BLKS mice were obtained from the Laboratory Animal Center, Academy of Military Medical Sciences (Beijing, China) and maintained under a 12-h light/12-h dark cycle at 24°C, with free access to mice chow and water. All experiments in this study were performed with the approval of the Animal Research Committee of Central Hospital of Zhumadian and according to the Guide for the Care and Use of Laboratory Animals from the National Institutes of Health.

TUG1 knockdown in vivo mediated by lentivirus

TUG1 small interfering RNA (siRNA) and control siRNA were constructed into lentiviral vector PHY-LV-KD5.1 (ThermoFisher Scientific, Waltham, MA) and then packed into lentivirus particles. Both wt and db/db mice were randomized into 3 groups (control, si-NC, and si-TUG1, n≥5 each group) and intratumorally injected with about 5×10^7 copies of the lentivirus with TUG1 siRNA or negative control, respectively. Approximately 30 μL phosphate-buffered saline (PBS) was administered to the control group. TUG1 knockdown in vivo was validated by RT-qPCR analysis.

Echocardiography and hemodynamics

The assessment of cardiac dysfunction in the diabetic myocardium was tested before sacrificing the mice. Echocardiography was performed using the 15-MHz linear array transducer interfaced with a Sequoia C256 (Acuson). The inherent measurement package of the ultrasound system was applied to measure the following parameters concerning the function and structure of the left ventricles: left ventricle ejection fraction (LVEF), left ventricular internal diameter diastole (LVIDd), left ventricular internal diameter systole (LVIDs), left ventricular posterior wall diastole (LVPWd), left ventricular posterior wall systole (LVPWs), and diastolic function (E/A ratio).

Mice hemodynamics were assessed as previously described [17]. The mice were anesthetized (1.5% isoflurane) sequentially and a high-fidelity Mikro-Tip catheter transducer (1.0 Fr, Model PVR-1030; Millar Instruments, Houston, Texas) was inserted into the right carotid artery and moved into the left ventricle. The maximal rates of increase and decrease in left ventricular pressure (+dp/dtmax, -dp/dtmin) were measured with a Millar PV System MPVS-300/400 (Millar Instruments, USA).

Biochemical examinations

Mice were fasted for 12 h prior to blood sample collection. The plasma was obtained by centrifugation and stored at -80°C until analysis. The lipid profile comprising of triglycerides, total cholesterol, high-density lipoprotein (HDL), and low-density lipoprotein (LDL) was determined for each animal. Serum lipid and fasting blood glucose (FBG), before transfection and 20 weeks after transfection, were measured enzymatically with commercial kits using the ACCU-CHEK Performa Blood Glucose Meter System (Roche, Auckland, New Zealand).

Masson's trichrome staining

From each mouse, one part of the heart was fixed in 10% formalin. After embedding in paraffin, 4 μm thickness sections were prepared and stained with Masson's trichrome stain to deter-

mine the fibrotic area with Image-ProPlus6 software (Media Cybernetics, Rockville, USA) as previously described [18].

Wheat germ agglutinin (WGA) staining

The cardiomyocyte diameter and length were measured by WGA staining and the cardiac myocyte size was analyzed using the ImageJ software (NIH, Bethesda, Rockville, MD, USA). The frozen heart sections were fixed with FAA (3.65% formaldehyde, 5% glacial acetic acid, and 50% alcohol) and washed with PBS three times. The slices were then incubated with 5 μg/ml WGA (Sigma) solubilized in PBS for 30 min shielded from light. After three washes with PBS, the slides were stained with DAPI (Sigma) for 2 min and fluorescent images were obtained using a research fluorescence microscope (Olympus America Inc., Center Valley, PA, USA).

Cell culture and treatment

Cardiomyocytes (CM) and non-cardiomyocytes (Non-CM) were isolated from mice, as previously described [19]. Mouse cardiomyocyte HL-1 cells were purchased from the American Type Culture Collection (ATCC, Manassas, VA) and cultured in the Claycomb medium (Sigma-Aldrich) supplemented with 10% fetal bovine serum (Gibco, Grand Island, NY, USA), and 1% U/mL penicillin and streptomycin, at 37°C in a humidified atmosphere of 5% CO_2. Briefly, cells were exposed to high glucose (HG, 30 mM) or normal glucose (normal, 5.5 mM) for 24 h and 48 h. Before cell infection, 1×10^5 HL-1 cells were cultured in 6-wells plates. Cells were incubated with 1×10^7 infectious units of lenti-si-TUG1 or lenti-si-NC in the culture medium. After 48 h, the medium containing viral particles was replaced with fresh medium. The infection efficiencies were validated by RT-qPCR analysis.

Dual-luciferase assay

According to TargetScan and Starbase information, the potential target of miR-499-5p was predicted. Fragments of the TUG1 3'-UTR containing the putative wild-type or mutant miR-499-5p binding sites were amplified and cloned into luciferase reporter constructs (Promega Biotech, USA) following the manufacturer's instruction. HL-1 cells were transfected with empty vehicle, miR-499-5p mimic (50 nM), mimic control (50 nM) using Lipofectamine 2000 agent according to the manufacturer's instructions. After 48 h of transfection, the activities were measured using a dual-luciferase reporter gene assay kit (Promega Biotech). Luciferase expression was analyzed by a Modulus single-tube multimode reader (Promega). Renilla luciferase activity was used as the internal control for normalization.

Immunofluorescence

The treated HL-1 cells were fixed with 4% paraformaldehyde and blocked with 4% BSA. Next, cells were incubated with β-actin antibody (1:500, Abcam) overnight at 4°C. The next day, cells were hybridized with DyLight 594 AffiniPure Goat Anti-Rabbit IgG (H+L) (CST) for 1 h at room temperature. The nuclei were stained with DAPI (Sigma). Cell images were captured by a fluorescence microscope at 200× magnification.

Western blotting

Proteins from cardiac tissues and cardiomyocytes were extracted using a lysis buffer containing phosphatase inhibitor cocktail II (Sigma-Aldrich) and centrifuged at 10,000 rpm for 10 min at 4°C. Subsequently, an equal protein load was separated by SDS-PAGE and the separated protein was transferred to PVDF membranes (Millipore, MA, USA). PVDF membranes were blocked in 5% fat-free milk at room temperature for 1 h and incubated with the primary antibodies against α-MHC (1:1000, Abcam), β-MHC (1:1000, Abcam) and β-actin (1:1000, Santa Cruz Biotechnology) overnight at 4°C. β-actin was used as an internal reference. Next, the membranes were incubated with goat anti-rabbit HRP-conjugated IgG (1:5000, Absin Bioscience Inc., shanghai, China) for 1 h at room temperature. The signals were detected by ECL agent (Beyotime, Jiangsu, China) on the XRS ChemiDoc system (BioRad) and analyzed by Quantity One software.

Real-time quantitative PCR (RT-qPCR)

In accordance with the manufacturer's instructions, TRIzol reagent (Invitrogen) was used to extract total RNA from cardiac tissues and cardiomyocytes. Later, the isolated RNA was reversely transcribed into cDNA, using the PrimeScript RT reagent Kit (Takara, Tokyo, Japan) and RT-qPCR was performed using

Table 1. The forward and reverse primers for real-time PCR

Genes		5'-3' primer sequence
TUG1	forward	TCAGCCCACCGTAACAAT
	reverse	CAAACTTCTCGGCGTCAT
ANP	forward	ACCTCCCGAAGCTACCTAAGT
	reverse	CAACCTTTTCAACGGCTCCAA
BNP	forward	TCACACAGGTTGTCCTCAGTGTGA
	reverse	GTCCCATCGATTAGGAGTGTTCAG
β-MHC	forward	ATGCGGGTCACGGCGCCCCGAAC
	reverse	TGGCCTTGCAGATCTGTGTCTCCCG
α-MHC	forward	ATGCGGGTCACGGCGCCCCGAAC
	reverse	TGGCCTTGCAGATCTGTGTCTCCCG
miR-499-5p	forward	TTAAGACTTGCAGTGATGTTT
	reverse	GAACATGTCTGCGTATCTC
β-actin	forward	GTCGTACCACAGGCATTGTGATGG
	reverse	GCAATGCCTGGGTACATGGTGG
U6	forward	CTCGCTTCGGCAGCACA
	reverse	AACGCTTCACGAATTTGCGT

SYBR Premix Ex Taq (TaKaRa). The PCR conditions were 95°C for 2 min, followed by 35 cycles of 95°C for 15 s, 60°C for 15 s, 72°C for 20 s, and 72°C for 7 min. A solubility curve was used to evaluate the reliability of the PCR results and the $2^{-\Delta\Delta CT}$ method [20] was used to calculate the relative expression of target genes. The primer sequences are listed in **Table 1**.

Statistical analysis

The statistical analysis was performed using SPSS version 22.0 software (IBM, Chicago, IL, USA). All experimental data were acquired from replicates and presented as mean ± standard deviation (SD). Student's t-test and one-way ANOVA were utilized to compare two or more groups. $P<0.05$ was considered statistically significant.

Results

Inhibition of TUG1 improves diastolic dysfunction in diabetic cardiomyopathy (DCM)

To investigate the expression and role of TUG1 in DCM, db/db mice were used as the animal model. As illustrated in **Figure 1A**, the expression of TUG1 was upregulated in heart of db/db mice when compared to the wide-type (wt; C57BLKS) mice; however, TUG1 was not upregulated in the lung, liver, and kidney. Furthermore, compared to non-cardiomyocyte (non-CM), TUG1 was specifically upregulated in cardiomyocyte (CM) of db/db mice (**Figure 1B**). Therefore, TUG1 knockdown was performed in wt and db/db mice by injecting lentivirus-mediated si-TUG1. The results demonstrated that the cardiac TUG1 level was significantly reduced in si-TUG1 treated mice when compared with si-NC treated mice (**Figure 1C**). Echocardiography was used to assess the effects of TUG1 silencing on cardiac function in DCM (**Figure 2A**). The results demonstrated that there was no significant change in LVEF (**Figure 2B**), LVIDd (**Figure 2C**), LVIDs (**Figure 2D**), LVPWs (**Figure 2E**), and LVPWd (**Figure 2F**) among the treated mice. This indicated that the TUG1 knockdown had no effect on systolic function in the early stage of DCM. Compared to the wt mice, db/db mice demonstrated a lower E/A ratio, which could be reversed by the TUG1 inhibition in db/db mice (**Figure 2G**). In addition, hemodynamic analysis revealed that there was no change in the level of +dp/dtmax among the treated mice (**Figure 2H**). However, the level of -dp/dtmax was decreased in db/db mice compared to wt mice and TUG1 silencing could abolish this observed decline (**Figure 2I**). Collectively, the data suggested that the TUG1 knockdown provided protection against diastolic dysfunction in DCM.

TUG1 inhibition has no effect on hyperglycemia and dyslipidemia in diabetic cardiomyopathy (DCM)

To determine the role of TUG1 on the metabolic characteristics of DCM, the blood glucose and lipid levels were measured. As shown in **Figure 3A** and **3B**, blood glucose was significantly increased in db/db mice compared to wt mice. However, TUG1 knockdown failed to influence blood glucose. Subsequently, a significant increase in the levels of TG, TC, LDL and decrease in the levels of HDL were observed in db/db mice compared to wt mice. Moreover, TUG1 inhibition in db/db mice demonstrated no influence on DCM-related dyslipidemia (**Figure 3C-F**).

Inhibition of TUG1 protects against cardiac hypertrophy in diabetic cardiomyopathy (DCM)

To further investigate the mechanisms underlying diastolic dysfunction, we observed that cardiac hypertrophy was increased in db/db mice compared to the wt mice. As expected, TUG1

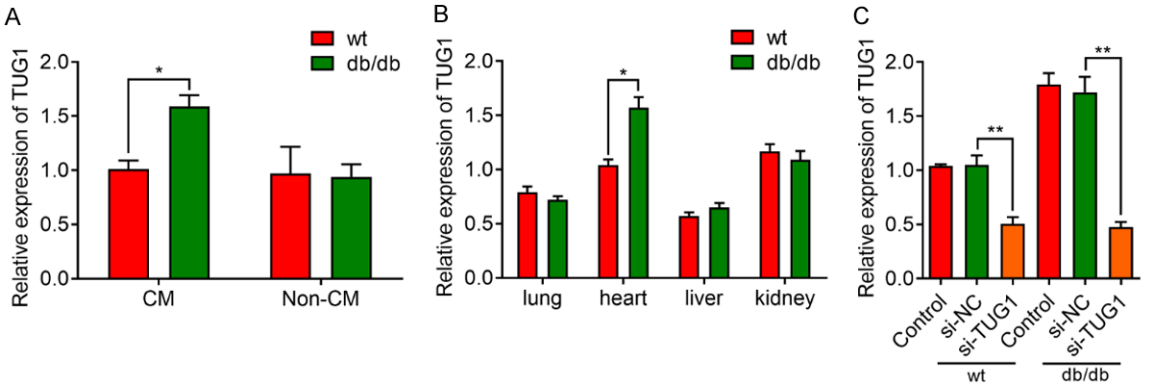

Figure 1. TUG1 is upregulated in cardiomyocytes from db/db mice with diabetic cardiomyopathy. A. Relative expression of TUG1 in isolated cardiomyocytes (CM) and non-cardiomyocytes (Non-CM) from wt (C57BLKS) mice or db/db mice. n=6 per group. B. Relative expression of TUG1 in different organs from wt or db/db mice. C. Relative expression of TUG1 in mice heart injected with lentiviral-mediated si-TUG1 or si-NC. *, P<0.05, vs. wt; **, P<0.05 vs. si-NC.

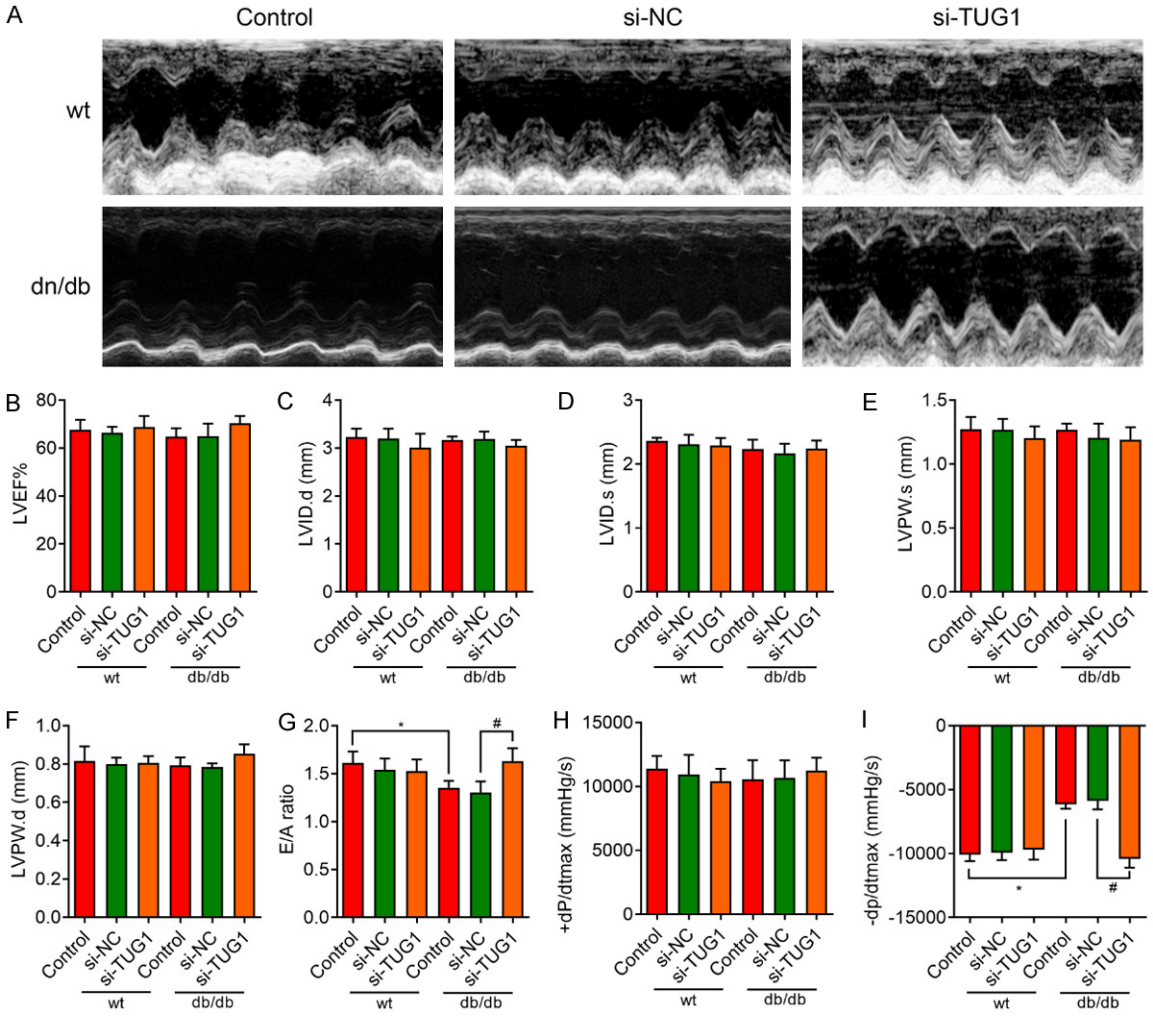

Figure 2. Inhibition of TUG1 protects against diastolic dysfunction in db/db mice. (A) Representative image of echocardiography of wt (C57BLKS) mice or db/db mice treated with lentiviral-mediated si-TUG1 or si-NC. (B-G) Echocardiographic analysis of treated wt or db/db mice. (B) left ventricle ejection fraction (LVEF), (C) left ventricular internal diameter diastole (LVIDd), (D) left ventricular internal diameter systole (LVIDs), (E) left ventricular posterior wall diastole (LVPWd), (F) left ventricular posterior wall systole (LVPWd), and (G) diastolic function (E/A ratio) were

quantitatively analyzed. However, no change in systolic function is observed after TUG1 knockdown in db/db mice. (H, I) Hemodynamic analysis of db/db mice and C57BL/Ks controls. (H) +dp/dtmax, maximal rate of the increase of left ventricular pressure; (I) -dp/dtmin, maximal rate of the decline of left ventricular pressure. n=6 per group. *, P<0.05, vs. control in wt group; #, P<0.05 vs. si-NC in db/db group.

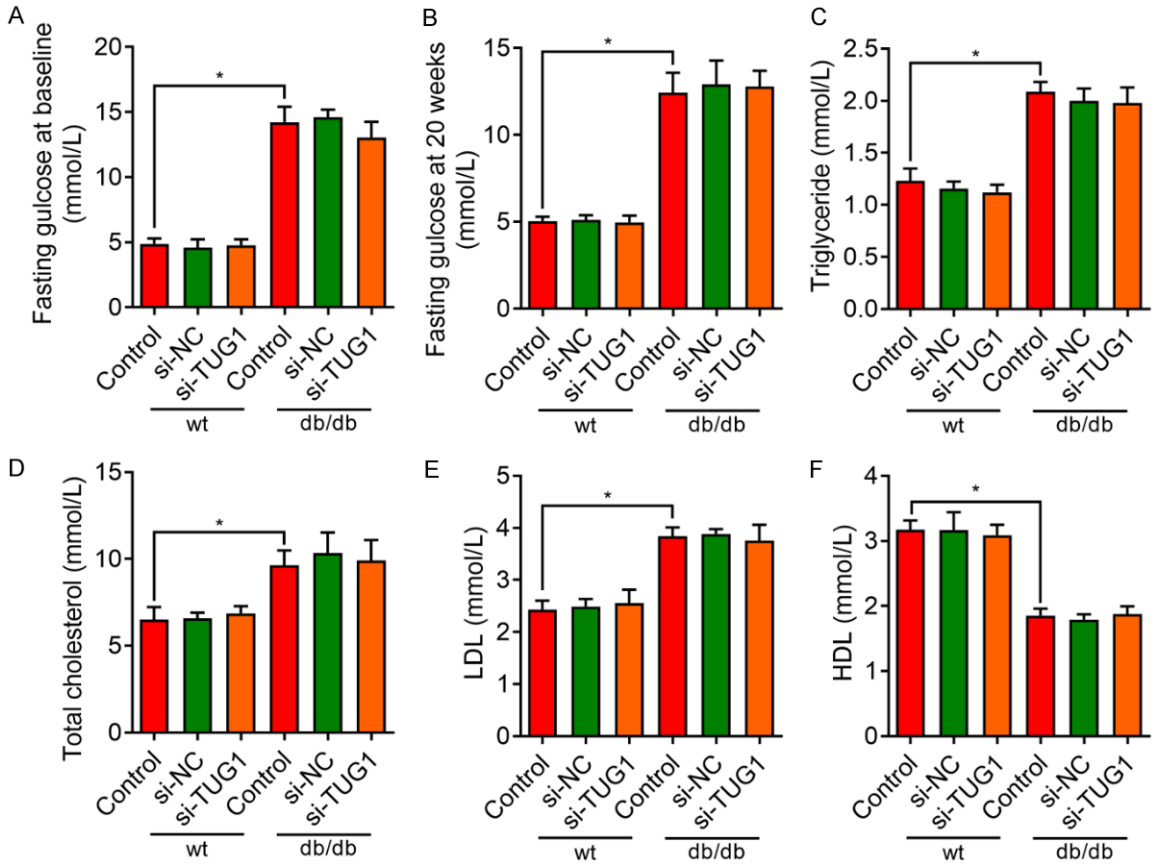

Figure 3. TUG1 inhibition has no influence on hyperglycemia and hyperlipidemia in db/db mice with diabetic cardiomyopathy. (A) Fasting glucose at baseline (before injection treatment) and (B) fasting glucose at 20 weeks after treatment were recorded in wt (C57BLKS) mice and db/db mice. However, knockdown of TUG1 showed no effects on hyperglycemia. (C-F) Changes in plasma lipid levels in wt and db/db mice with or without knockdown of TUG1. TUG1 silencing demonstrates no influence on the levels of plasma (C) TG, (D) TC, (E) LDL and (F) HDL in mice. *, P<0.05, vs. control in wt group.

knockdown significantly decreased cardiac hypertrophy in db/db mice, as detected by WGA staining (**Figure 4A**). Furthermore, the expression of hypertrophy markers such as ANP, BNP, and β-/α-MHC ratio was significantly increased in db/db mice compared to wt mice. TUG1 inhibition markedly reduced the above-mentioned markers, both in wt and db/db mice (**Figure 4B-D**). In addition, Masson trichrome staining exhibited greater fibrosis in db/db mice compared to the wt mice. Notably, TUG1 knockdown markedly reduced the fibrotic area in db/db mice (**Figure 4E**). Collectively, these results indicated that TUG1 inhibition mitigated cardiac hypertrophy in DCM.

Inhibition of TUG1 attenuates the hypertrophic response in high glucose (HG)-treated CMs

To further validate the function of TUG1 *in vitro*, HG-mediated mouse CMs HL-1 cells were selected for analysis. HL-1 cells treated with HG for 24 and 48 h demonstrated a significant upregulation in TUG1 expression (**Figure 5A**). To further confirm the function of TUG1 in cardiomyocytes, we inhibited TUG1 expression in HL-1 cells by infecting with lentivirus-mediated si-TUG1. Subsequently, RT-qPCR validated that the expression of TUG1 was notably decreased in the si-TUG1 group compared to the si-NC group (**Figure 5B**). HG stimulation for 48 h

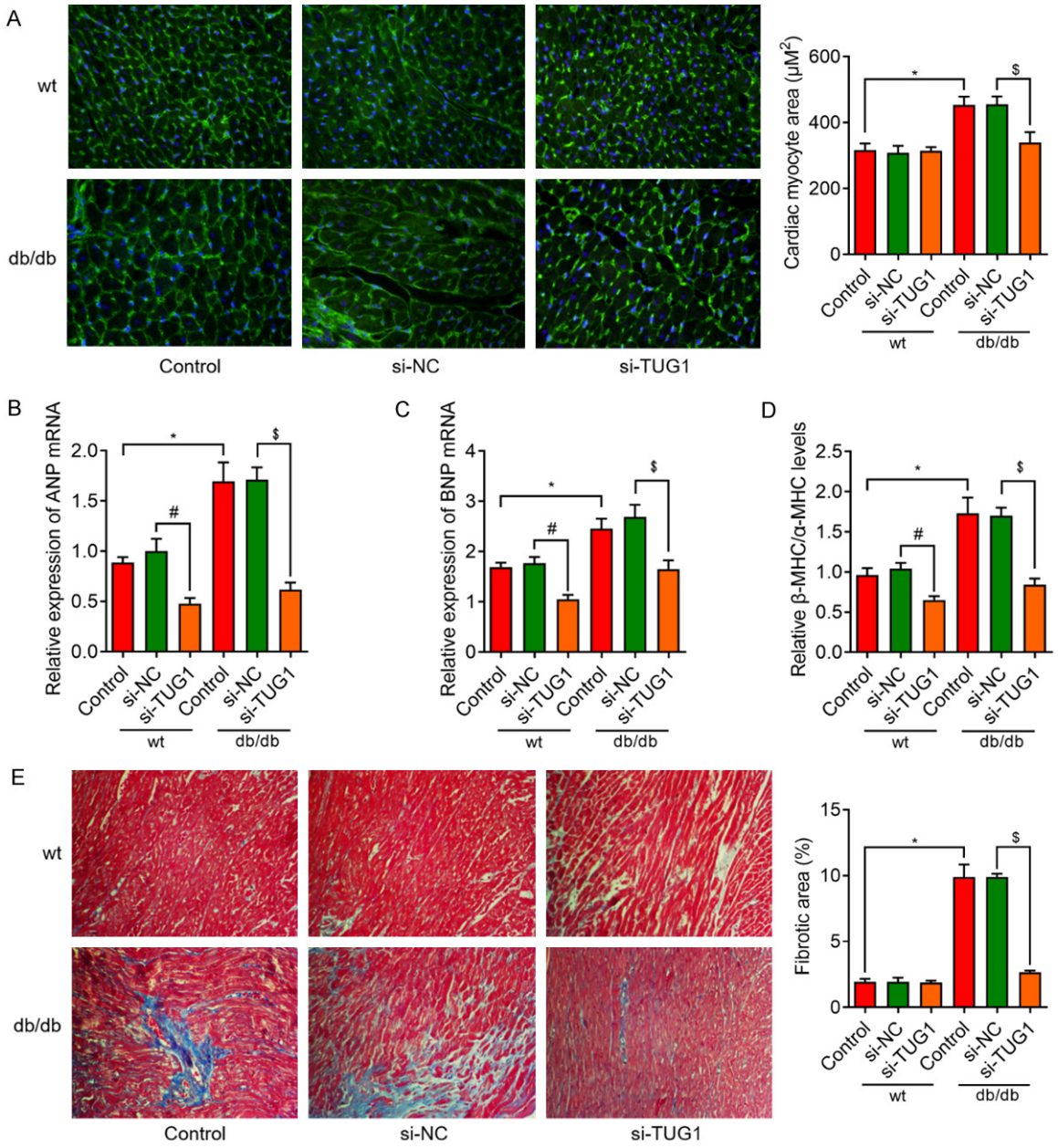

Figure 4. Inhibition of TUG1 alleviates cardiac hypertrophy in diastolic dysfunction db/db mice. A. WGA staining of left ventricular tissue from treated mice (wt mice and db/db mice with or without knockdown of TUG1) for cardiac hypertrophy determination. Magnification at 200×. TUG1 knockdown decreases the cardiomyocyte size in db/db mice. B-D. Relative expression of ANP, BNP, and β-MHC/α-MHC in cardiac tissues from wt or db/db mice. TUG1 knockdown decreases the levels of cardiac hypertrophy markers. E. Representative images of Masson's trichrome show that TUG1 knockdown decreases the fibrotic area in db/db mice. *P<0.05, vs. control in wt group; $P<0.05 vs. si-NC in db/dbt group.

increased the HL-1 cell size; TUG1 inhibition remarkably alleviated the increased HL-1 cell size reflecting cardiac hypertrophy in vitro (**Figure 5C**, **5D**). Similarly, the expression of the β-MHC protein in HG treated HL-1 cells was increased, whereas α-MHC expression in treated HL-1 cells was unaltered. TUG1 inhibition abrogated the increase in β-MHC (**Figure 5E-G**). Collectively, the data suggested that TUG1 knockdown inhibited the switch in the isoform arrangement from α- to β-MHC, alleviating the development of cardiac hypertrophy.

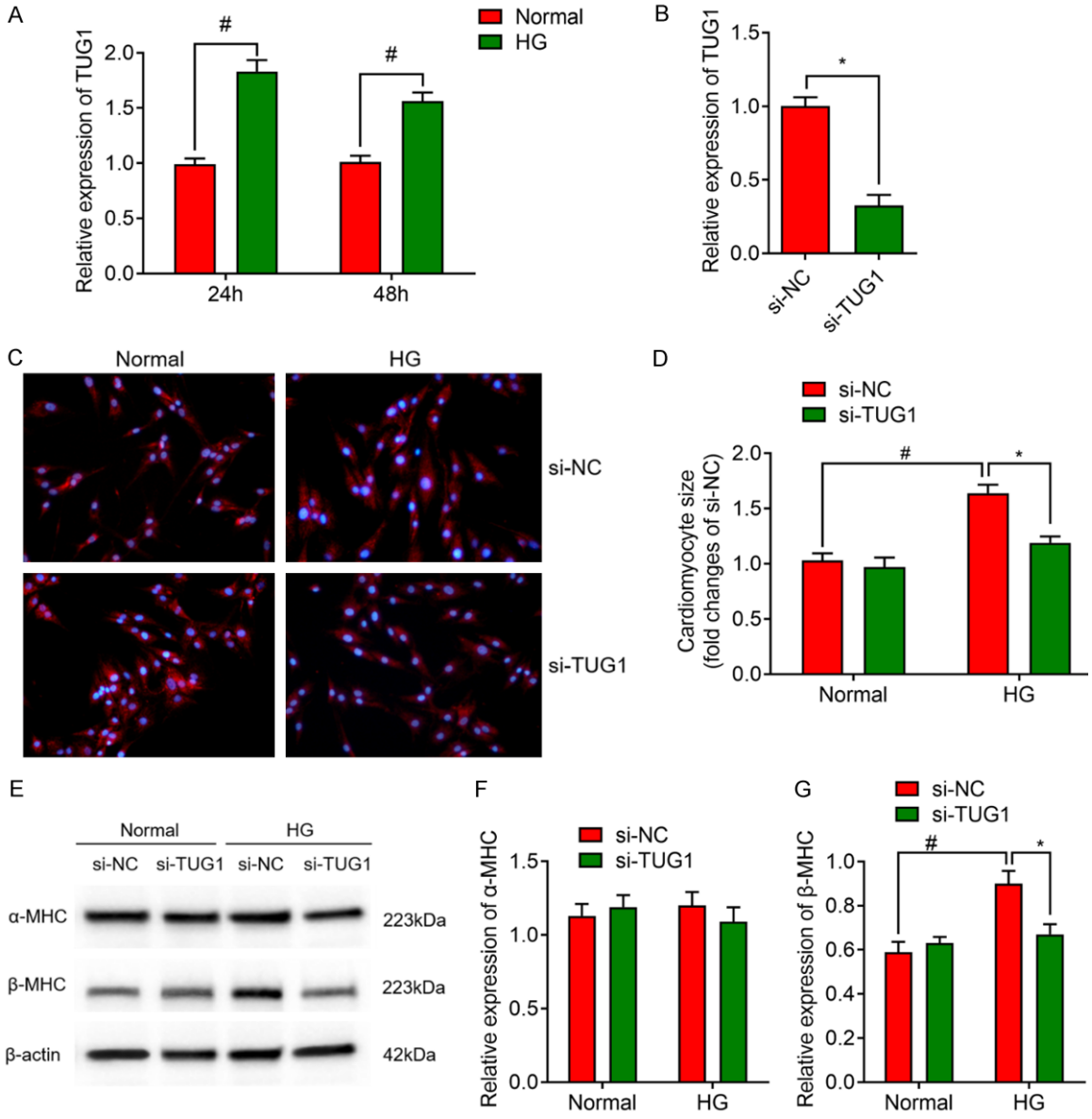

Figure 5. TUG1 inhibition attenuates cardiac hypertrophy in high glucose (HG)-induced HL-1 mouse cardiomyocyte. A. The expression of TUG1 in normal and HG treated HL-1 cells at 24 and 48 h, as detected by RT-qPCR analysis. B. TUG1 inhibition in HL-1 cells was performed by infection with lentiviral-mediated si-TUG1. C, D. Representative fluorescence microscopy images of HL-1 cells staining with β-actin, reflecting the changes in cardiomyocytes size. TUG1 knockdown decreases the cell size of HG-treated cardiomyocytes. E-G. Relative expression of α-MHC and β-MHC in HL-1 cells with TUG1 silencing under normal and HG conditions. TUG1 silencing decreases β-MHC protein expression in HG-treated cardiomyocytes. *P<0.05, vs. si-NC in the HG group; #P<0.05 vs. si-NC in the normal group.

MiR-499-5p is a direct target of TUG1

To explore the molecular mechanisms underlying the pro-hypertrophic effect of TUG1, we used online prediction softwares, TargetScan and Starbase, to select a potential miRNA. We selected a miRNA reportedly involved in the process of cardiomyocyte injury [21-23]. As shown in **Figure 6A**, we compared the sequences of TUG1 and miR-499-5p and noticed that TUG1 contained three binding sites of miR-499-5p. In addition, we observed that miR-499-5p was decreased in CM of db/db mice (**Figure 6B**) and HG treated HL-1 cells (**Figure 6C**). Subsequent experiments demonstrated that TUG1 inhibition increased the expression of miR-499-5p under normal and HG conditions (**Figure 6D**). Furthermore, the overexpres-

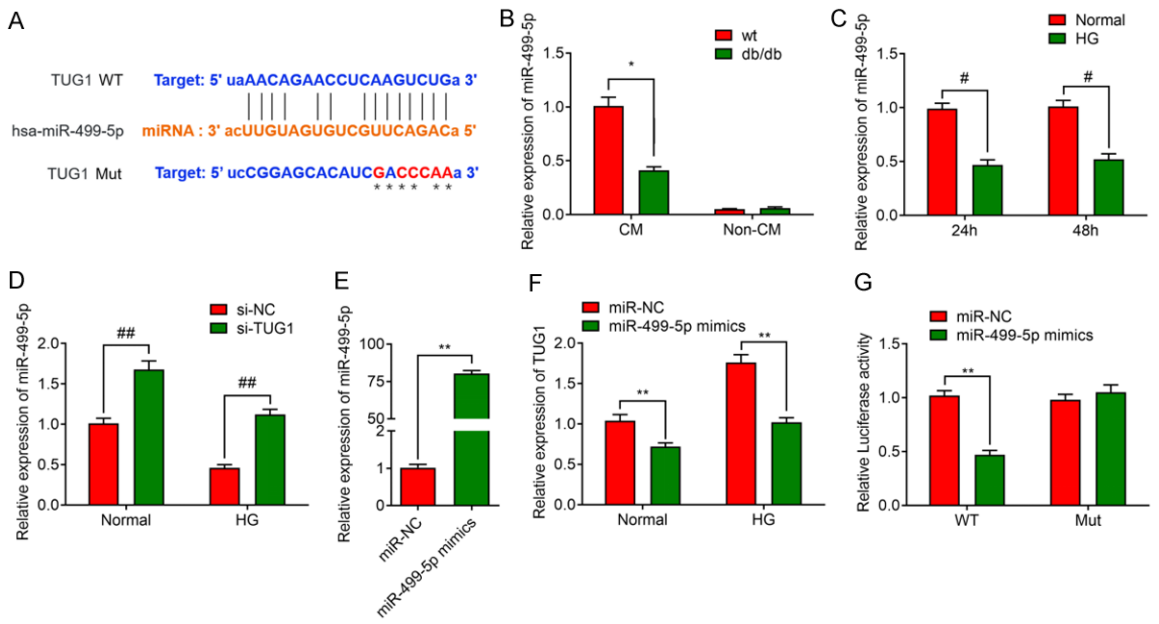

Figure 6. MiR-499-5p is a direct target of TUG1. A. The predicted complementary binding sites for TUG1 and miR-499-5p at 3'-UTR. Wild-type (WT) and mutant-type (Mut) TUG1 3'-UTR were constructed. B. Relative expression of miR-499-5p in isolated cardiomyocytes (CM) and non-cardiomyocytes (Non-CM) from wt (C57BLKS) mice or db/db mice. n=6 per group. C. The expression of miR-499-5p in normal and HG treated HL-1 cells at 24 and 48 h, as detected by RT-qPCR analysis. D. Relative expression of miR-499-5p in HL-1 cells is significantly upregulated after TUG1 silencing under normal or HG conditions. E. Overexpression of miR-499-5p was achieved by transfected with miR-499-5p mimics. F. Relative expression of TUG1 in HL-1 cells is downregulated when miR-499-5p is overexpressed under normal or HG conditions. G. HL-1 cells were co-transfected with TUG1-WT, TUG1-Mut, and miR-499-5p or miR-NC. The luciferase activity was analyzed in each group; however, there is no change in Mut-TUG1. $^{*}P<0.05$, vs. wt group; $^{**}P<0.05$ vs. miR-NC group; $^{\#}P<0.05$ vs. normal group; $^{\#\#}P<0.05$, vs. si-NC group.

sion of miR-499-5p in HL-1 cells confirmed the relationship between TUG1 and miR-499-5p (**Figure 6E**). In contrast, we observed that the overexpression of miR-499-5p reduced TUG1 expression both under normal and HG conditions (**Figure 6F**). Furthermore, the dual-luciferase reporter assay revealed that miR-499-5p significantly suppressed luciferase activity of TUG1 wild-type (WT), while not influencing TUG1 mutant type (Mut) compared to miR-NC group (**Figure 6G**). These results indicated that miR-4pp-5p could directly target 3'UTR of TUG1 to regulate expression.

TUG1 directly interacted with miR-499-5p to participate in cardiac hypertrophy

Next, we investigated whether TUG1 exerts its role by targeting miR-499-5p in cardiac hypertrophy. As depicted in **Figure 7A** and **7B**, the co-transfection of miR-499-5p abated the inhibitory effects of TUG1 silencing on the HG-induced increase in the size of HL-1 cells. Additionally, although the overexpression of miR-499-5p had no influence on the expression of α-MHC, this overexpression reversed the β-MHC decrease observed in TUG1 silenced HL-1 cells (**Figure 7C-E**). Our results demonstrated that TUG1 participated in HG-mediated cardiac hypertrophy by targeting miR-499-5p.

Discussion

In diabetic stress, cardiac hypertrophy is an important compensatory mechanism of the heart in response to persistent hyperglycemia. Initially, in order to normalize wall stress and preserve contractile performance, the heart undergoes cardiac remodeling and pathological growth of the cardiomyocytes. Nevertheless, chronic hyperglycemia stimuli leads to hypertrophy and cardiac dysfunction [24, 25]. Although a variety of pathways provide coordinated control during cardiac hypertrophy, the associated molecular mechanisms are yet to be established.

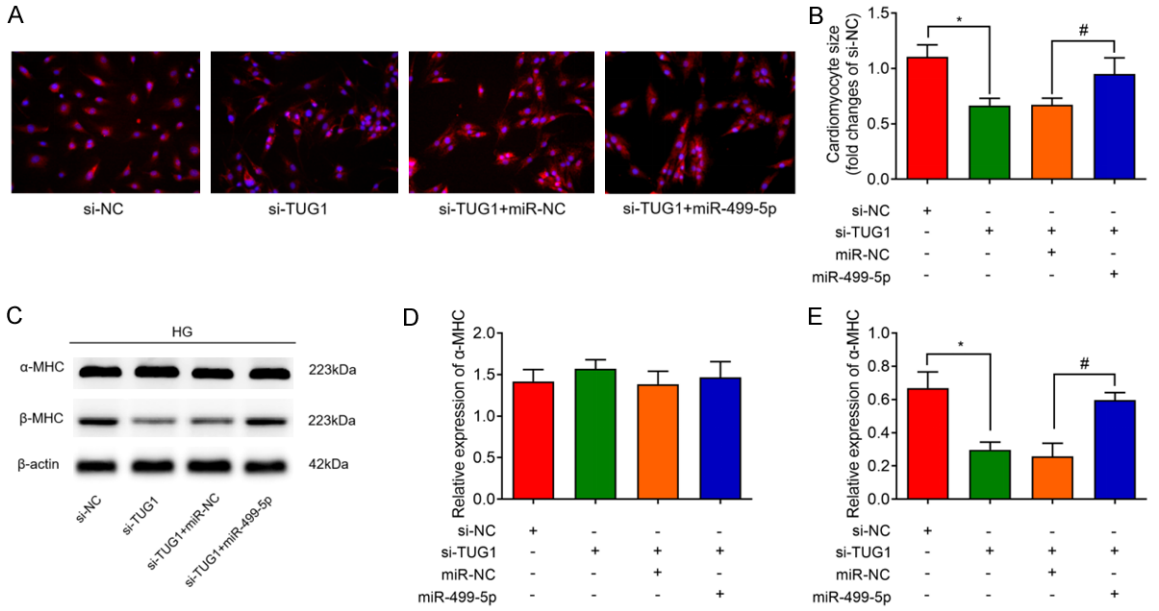

Figure 7. TUG1/miR-499-5p axis is involved in the regulation of high glucose (HG)-mediated cardiac hypertrophy. A, B. Representative fluorescence microscopy images of HL-1 cells staining with β-actin, reflecting the changes in cardiomyocyte size after treatment with si-TUG1, si-NC, miR-499-5p mimics or miR-NC. Overexpression of miR-499-5p partly reverses the inhibitory effects of TUG1 silencing on HG-induced cardiomyocytes size. C-E. Relative expression of α-MHC and β-MHC in HL-1 cells with the inhibition of TUG1 and/or overexpression of miR-499-5p under HG condition. Overexpression of miR-499-5p could reverse the TUG1 silencing induced decrease in β-MHC protein expression in HG-treated cardiomyocytes. *P<0.05, vs. si-NC group; #P<0.05 vs. si-TUG1+miR-NC group.

LncRNA plays a significant role in several biological processes including diabetes, cardiovascular diseases, and related complications. However, the relationship between TUG1 and DCM-related cardiac hypertrophy is unknown. Here, our data demonstrated that the expression of the TUG1 was significantly increased in the CM of diabetic mice and HG-treated CM. TUG1 inhibition ameliorated cardiac hypertrophy by targeting miR-499-5p, thus improving cardiac function in DCM. This is the first study to illuminate the effect of TUG1 on cardiac hypertrophy in DCM.

Previous studies have reported the involvement of TUG1 in cardiovascular disease. Shi et al. identified that TUG1 was highly expressed in the aorta of spontaneously hypertensive rats and promoted the proliferation and migration of vascular smooth muscle cells by regulating miR-145-5p [26]. Similarly, Li et al. observed that TUG1 was highly expressed in serum samples from atherosclerotic patients, promoting the proliferation of atherosclerosis by suppressing PTEN activity [27]. In addition, TUG1 was reportedly upregulated in myocardial infarction and TUG1 knockdown promoted hypoxia-induced cell injury by upregulating miR-124 [28]. In contrast, a recent study by Su et al. demonstrated that the inhibition of lncRNA TUG1 upregulated miR-142-3p, ameliorating myocardial injury during ischemia and reperfusion [29]. Therefore, the exact role of TUG1 in cardiovascular disease necessitates further examination. We also noticed that TUG1 participated in HG-mediated diabetic nephropathy by activating endoplasmic reticulum stress and subsequent excessive podocyte apoptosis [30]. To date, no investigation has reported on the expression levels and the biological function of TUG1 in DCM. In our novel study, we demonstrated that TUG1 was upregulated in diabetic CM, but not in the lung, kidney, and liver. Together with the increased TUG1 expression in HG-induced podocyte, these observations indicated that the regulation of TUG1 was tissue-specific. However, more studies are needed to confirm this hypothesis. This study identified that knockdown of TUG1 alleviated cardiac hypertrophy and fibrotic area in DCM. Furthermore, we identified that TUG1 inhibition significantly improved diastolic dysfunction in DCM. A previous study reported that the inhibi-

tion of lncRNA maternally expressed gene 3 decreased cardiac fibrosis and improved the diastolic performance by regulating the production of matrix metalloproteinase-2 [31]. Similarly, Liu et al. identified that the inhibition of lncRNA MIRT1 significantly alleviated the cardiac function damage and cardiomyopathy in aged diabetic rats [32]. Along with our data, these results suggested the effective regulatory role of lncRNAs in DCM-related cardiac dysfunction.

A range of miRNAs have been predicted as the potential targets of TUG1 such as miR-145-5p [26], miR-204-5p [33], and miR-29c [34]. Using online prediction software, we hypothesized that miR-499-5p was a TUG1 target. We focused on miR-499-5p as it has been known to be expressed in CM exclusively [35]. Although studies reported that miR-499-5p was remarkably increased in the plasma sample of patients with acute myocardial infarction [22, 36], it was decreased in hypoxia-induced H9C2 cells. Moreover, the overexpression of miR-499-5p attenuated hypoxia-mediated cell injury [37]. The changes in miR-499-5p in CM following HG treatment and its role in DCM need to be thoroughly explored. In the present study, we first identified that miR-499-5p was significantly downregulated in diabetic CM and HG-treated CM. The dual-luciferase reporter assay demonstrated that the combination of TUG1 and miR-499-5p decreased luciferase activities, indicating the complementary binding at 3'-UTR. The overexpression of miR-499-5p could reverse the inhibitory effects of TUG1 silencing on HG-mediated cardiac hypertrophy. Furthermore, our results contributed to evidence regarding the regulation of miR-499-5p in CM injury.

Nevertheless, our study has certain limitations. First, we failed to evaluate TUG1 expression in patients with DCM. A recent study observed that TUG1 was upregulated in the plasma samples of patients with prostate cancer [38] and osteosarcoma [39]. These data confirmed that elevated TUG1 could exist stably in the plasma and be detected, prompting us to further investigate the predictive ability of TUG1 in early stages of DCM in future investigations. Besides, we only observed that TUG1 inhibition attenuated cardiac hypertrophy and improved cardiac function in DCM mice. However, whether TUG1 overexpression could activate cardiac hypertrophy needs to be evaluated. Finally, the target genes of miR-499-5p were not identified in the current study and further investigations are imperative.

Collectively, our data demonstrate that TUG1 was upregulated in DCM and inhibition of TUG1 protects against DCM-induced diastolic dysfunction by regulating miR-499-5p. The results suggest that TUG1 might be a potential therapeutic target to alleviate DCM.

Acknowledgements

This work was supported by the key scientific and technological plan funding project of Zhumadian Central Hospital (No. 16604) and the Natural Science Fund of Henan Province (grant no. HN2017ZA043).

Disclosure of conflict of interest

None.

Address correspondence to: Lei Zhao, Department of Ultrasonic, Central Hospital of Zhumadian, No. 747, Zhonghua Road, Zhumadian 463000, Henan Province, China. E-mail: zhaol_000@163.com

References

[1] Dillmann WH. Diabetic cardiomyopathy. Circ Res 2019; 124: 1160-1162.
[2] Jia G, Whaley-Connell A and Sowers JR. Diabetic cardiomyopathy: a hyperglycaemia- and insulin-resistance-induced heart disease. Diabetologia 2018; 61: 21-28.
[3] Parim B, Sathibabu Uddandrao VV and Saravanan G. Diabetic cardiomyopathy: molecular mechanisms, detrimental effects of conventional treatment, and beneficial effects of natural therapy. Heart Fail Rev 2019; 24: 279-299.
[4] Borghetti G, von Lewinski D, Eaton DM, Sourij H, Houser SR and Wallner M. Diabetic cardiomyopathy: current and future therapies. Beyond glycemic control. Front Physiol 2018; 9: 1514.
[5] Jiang X and Zhang F. Long noncoding RNA: a new contributor and potential therapeutic target in fibrosis. Epigenomics 2017; 9: 1233-1241.
[6] Feng SD, Yang JH, Yao CH, Yang SS, Zhu ZM, Wu D, Ling HY and Zhang L. Potential regulatory mechanisms of lncRNA in diabetes and its complications. Biochem Cell Biol 2017; 95: 361-367.
[7] Ma C, Luo H, Liu B, Li F, Tschope C and Fa X. Long noncoding RNAs: a new player in the pre-

vention and treatment of diabetic cardiomyopathy? Diabetes Metab Res Rev 2018; 34: e3056.
[8] Zhang M, Gu H, Chen J and Zhou X. Involvement of long noncoding RNA MALAT1 in the pathogenesis of diabetic cardiomyopathy. Int J Cardiol 2016; 202: 753-755.
[9] Feng Y, Xu W, Zhang W, Wang W, Liu T and Zhou X. LncRNA DCRF regulates cardiomyocyte autophagy by targeting miR-551b-5p in diabetic cardiomyopathy. Theranostics 2019; 9: 4558-4566.
[10] Zheng D, Zhang Y, Hu Y, Guan J, Xu L, Xiao W, Zhong Q, Ren C, Lu J, Liang J and Hou J. Long noncoding RNA Crnde attenuates cardiac fibrosis via Smad3-Crnde negative feedback in diabetic cardiomyopathy. FEBS J 2019; 286: 1645-1655.
[11] Xue YN, Yan Y, Chen ZZ, Chen J, Tang FJ, Xie HQ, Tang SJ, Cao K, Zhou X, Wang AJ and Zhou JD. LncRNA TUG1 regulates FGF1 to enhance endothelial differentiation of adipose-derived stem cells by sponging miR-143. J Cell Biochem 2019; 120: 19087-19097.
[12] Yu G, Zhou H, Yao W, Meng L and Lang B. lncRNA TUG1 promotes cisplatin resistance by regulating CCND2 via epigenetically silencing miR-194-5p in bladder cancer. Mol Ther Nucleic Acids 2019; 16: 257-271.
[13] Zhuang S, Liu F and Wu P. Upregulation of long noncoding RNA TUG1 contributes to the development of laryngocarcinoma by targeting miR-145-5p/ROCK1 axis. J Cell Biochem 2019; 120: 13392-13402.
[14] Shi H, Dong Z and Gao H. LncRNA TUG1 protects against cardiomyocyte ischaemia reperfusion injury by inhibiting HMGB1. Artif Cells Nanomed Biotechnol 2019; 47: 3511-3516.
[15] Zhang H, Li H, Ge A, Guo E, Liu S and Zhang L. Long non-coding RNA TUG1 inhibits apoptosis and inflammatory response in LPS-treated H9c2 cells by down-regulation of miR-29b. Biomed Pharmacother 2018; 101: 663-669.
[16] Duan LJ, Ding M, Hou LJ, Cui YT, Li CJ and Yu DM. Long noncoding RNA TUG1 alleviates extracellular matrix accumulation via mediating microRNA-377 targeting of PPARgamma in diabetic nephropathy. Biochem Biophys Res Commun 2017; 484: 598-604.
[17] Sciarretta S, Yee D, Nagarajan N, Bianchi F, Saito T, Valenti V, Tong M, Del Re DP, Vecchione C, Schirone L, Forte M, Rubattu S, Shirakabe A, Boppana VS, Volpe M, Frati G, Zhai P and Sadoshima J. Trehalose-induced activation of autophagy improves cardiac remodeling after myocardial infarction. J Am Coll Cardiol 2018; 71: 1999-2010.
[18] Li TT, Jia LX, Zhang WM, Li XY, Zhang J, Li YL, Li HH, Qi YF and Du J. Endoplasmic reticulum stress in bone marrow-derived cells prevents acute cardiac inflammation and injury in response to angiotensin II. Cell Death Dis 2016; 7: e2258.
[19] Louch WE, Sheehan KA and Wolska BM. Methods in cardiomyocyte isolation, culture, and gene transfer. J Mol Cell Cardiol 2011; 51: 288-298.
[20] Livak KJ and Schmittgen TD. Analysis of relative gene expression data using real-time quantitative PCR and the 2(-Delta Delta C(T)) Method. Methods 2001; 25: 402-408.
[21] Pinchi E, Frati P, Aromatario M, Cipolloni L, Fabbri M, La Russa R, Maiese A, Neri M, Santurro A, Scopetti M, Viola RV, Turillazzi E and Fineschi V. miR-1, miR-499 and miR-208 are sensitive markers to diagnose sudden death due to early acute myocardial infarction. J Cell Mol Med 2019; 23: 6005-6016.
[22] Zhou R, Huang W, Fan X, Liu F, Luo L, Yuan H, Jiang Y, Xiao H, Zhou Z, Deng C and Dang X. miR-499 released during myocardial infarction causes endothelial injury by targeting alpha7-nAchR. J Cell Mol Med 2019; 23: 6085-6097.
[23] Zhu Z and Zhao C. LncRNA AK139128 promotes cardiomyocyte autophagy and apoptosis in myocardial hypoxia-reoxygenation injury. Life Sci 2019; 116705.
[24] Rawal S, Nagesh PT, Coffey S, Van Hout I, Galvin IF, Bunton RW, Davis P, Williams MJA and Katare R. Early dysregulation of cardiac-specific microRNA-208a is linked to maladaptive cardiac remodelling in diabetic myocardium. Cardiovasc Diabetol 2019; 18: 13.
[25] Yang F, Qin Y, Lv J, Wang Y, Che H, Chen X, Jiang Y, Li A, Sun X, Yue E, Ren L, Li Y, Bai Y and Wang L. Silencing long non-coding RNA Kcnq1ot1 alleviates pyroptosis and fibrosis in diabetic cardiomyopathy. Cell Death Dis 2018; 9: 1000.
[26] Shi L, Tian C, Sun L, Cao F and Meng Z. The lncRNA TUG1/miR-145-5p/FGF10 regulates proliferation and migration in VSMCs of hypertension. Biochem Biophys Res Commun 2018; 501: 688-695.
[27] Li FP, Lin DQ and Gao LY. LncRNA TUG1 promotes proliferation of vascular smooth muscle cell and atherosclerosis through regulating miRNA-21/PTEN axis. Eur Rev Med Pharmacol Sci 2018; 22: 7439-7447.
[28] Jiang N, Xia J, Jiang B, Xu Y and Li Y. TUG1 alleviates hypoxia injury by targeting miR-124 in H9c2 cells. Biomed Pharmacother 2018; 103: 1669-1677.
[29] Su Q, Liu Y, Lv XW, Ye ZL, Sun YH, Kong BH and Qin ZB. Inhibition of lncRNA TUG1 upregulates miR-142-3p to ameliorate myocardial injury during ischemia and reperfusion via targeting HMGB1- and Rac1-induced autophagy. J Mol Cell Cardiol 2019; 133: 12-25.

[30] Shen H, Ming Y, Xu C, Xu Y, Zhao S and Zhang Q. Deregulation of long noncoding RNA (TUG1) contributes to excessive podocytes apoptosis by activating endoplasmic reticulum stress in the development of diabetic nephropathy. J Cell Physiol 2019; [Epub ahead of print].

[31] Piccoli MT, Gupta SK, Viereck J, Foinquinos A, Samolovac S, Kramer FL, Garg A, Remke J, Zimmer K, Batkai S and Thum T. Inhibition of the cardiac fibroblast-enriched lncRNA Meg3 prevents cardiac fibrosis and diastolic dysfunction. Circ Res 2017; 121: 575-583.

[32] Liu Y, Wang T, Zhang M, Chen P and Yu Y. Down-regulation of myocardial infarction associated transcript 1 improves myocardial ischemia-reperfusion injury in aged diabetic rats by inhibition of activation of NF-kappaB signaling pathway. Chem Biol Interact 2019; 300: 111-122.

[33] Yu C, Li L, Xie F, Guo S, Liu F, Dong N and Wang Y. LncRNA TUG1 sponges miR-204-5p to promote osteoblast differentiation through upregulating Runx2 in aortic valve calcification. Cardiovasc Res 2018; 114: 168-179.

[34] Zhu Y, Feng Z, Jian Z and Xiao Y. Long noncoding RNA TUG1 promotes cardiac fibroblast transformation to myofibroblasts via miR29c in chronic hypoxia. Mol Med Rep 2018; 18: 3451-3460.

[35] Agiannitopoulos K, Pavlopoulou P, Tsamis K, Bampali K, Samara P, Nasioulas G, Mertzanos G, Babalis D and Lamnissou K. Expression of miR-208b and miR-499 in Greek patients with acute myocardial infarction. In Vivo 2018; 32: 313-318.

[36] Zhao J, Yu H, Yan P, Zhou X, Wang Y and Yao Y. Circulating microRNA-499 as a diagnostic biomarker for acute myocardial infarction: a meta-analysis. Dis Markers 2019; 2019: 6121696.

[37] Shi Y, Han Y, Niu L, Li J and Chen Y. MiR-499 inhibited hypoxia/reoxygenation induced cardiomyocytes injury by targeting SOX6. Biotechnol Lett 2019; 41: 837-847.

[38] Xu T, Liu CL, Li T, Zhang YH and Zhao YH. LncRNA TUG1 aggravates the progression of prostate cancer and predicts the poor prognosis. Eur Rev Med Pharmacol Sci 2019; 23: 4698-4705.

[39] Ma B, Li M, Zhang L, Huang M, Lei JB, Fu GH, Liu CX, Lai QW, Chen QQ and Wang YL. Upregulation of long non-coding RNA TUG1 correlates with poor prognosis and disease status in osteosarcoma. Tumour Biol 2016; 37: 4445-4455.